Short communication

Fast redox of composite electrode of nitroxide radical polymer and carbon with polyacrylate binder

Shinichi Komaba [a,*], Tatsuya Tanaka [a], Tomoaki Ozeki [a], Takayuki Taki [b], Hiroaki Watanabe [b], Hiroyuki Tachikawa [b]

[a] Department of Applied Chemistry, Tokyo University of Science, 1-3 Kagurazaka, Shinjuku, Tokyo 162-0825, Japan
[b] Advanced Materials R & D Laboratory, ADEKA Co., Ltd., 7-2-34 Higashiogu, Arakawa, Tokyo 116-8553, Japan

ARTICLE INFO

ABSTRACT

For organic radical batteries, poly(2,2,6,6-tetramethylpiperidinyloxy-4-yl methacrylate) (PTMA) has been reported as a promising positive electrode material. The PTMA/C composite electrode prepared with polyacrylate binder demonstrated the fast redox performance for the application to aprotic secondary batteries. When the variation in discharge capacities of the PTMA/C composite electrode was tested galvanostatically at $20C$ rates, the electrode retained 96% of the initial capacity after 1000 cycles. This is attributed to the fact that the redox of PTMA is a simple reaction to form the oxoammonium salt doped with ClO_4^- anions in the electrolyte. When the PTMA/C composite electrode was discharged at different C rates, the electrode retained 81% of the theoretical capacity even at $50C$ rates. This remarkably high rate capability originates from the fast electron-transfer kinetic of the 2,2,6,6-tetramethylpiperidine-N-oxyl (so-called TEMPO) radical, partially jelled polyacrylate binder, and the improved conductivity throughout the electrode by thoroughly mixing with carbon.

© 2009 Elsevier B.V. All rights reserved.

1. Introduction

Organic radical compounds, which possess unpaired electrons, are known as intermediates in photochemical and thermal reactions. Generally, they are unstable and their lifetime is very short, so they are decomposed by dimerization and reactions with other molecules, solvents, or molecular oxygen because of their high reactivity. Thus it is difficult to isolate organic radical compounds usually. However, some organic radical compounds can be isolated and exist stably for appreciable duration of lifetime under ambient laboratory conditions. The well-known stable nitroxide radical compound, 2,2,6,6-tetramethylpiperidine-N-oxyl (TEMPO), is highly stabilized by the steric protection around the radical center and its resonance structures involving the unpaired electron.

The redox reactions of nitroxide radicals can be classified into two types as shown in Fig. 1. One is p-type redox reaction. In the p-type reaction, nitroxide radical is oxidized to an oxoammonium cation and forms an ionic pair with a counter anion (A^-, e.g. an anion in electrolyte) to keep its electrical neutrality. And the other is n-type redox reaction. In the n-type reaction, nitroxide radical is reduced to an aminoxy anion and forms an ionic pair with a counter cation (C^+, e.g. a cation in electrolyte) similarly.

Rechargeable organic radical batteries are operated on the basis of redox reactions of these stable organic radicals which show high redox activity and possess high-power capability. Recently, poly(2,2,6,6-tetramethylpiperidinyloxy-4-yl methacrylate) (PTMA) has been reported as a promising positive electrode material [1–10]. PTMA exhibits a highly reversible p-type behavior around 3–4 V vs. Li, and its theoretical capacity reaches at 111 mAh g^{-1}. In addition, this compound shows fast redox kinetic and long cycle life, but because of its poor electrical conductivity it needs a large quantity of conductive assistance to sufficiently reduce resistance within electrode. In recent reports, several ways were reported to improve its electrical conduction, e.g. mixing PTMA with graphite [1] and covering carbon fibers as conductive assistants with PTMA [8]. In this study, we report the preparation of the thoroughly mixed PTMA/carbon composite electrode with novel polyacrylate binders and the PTMA composite electrode demonstrated the fast redox performance which is appliable to aprotic secondary batteries or redox capacitors.

2. Experimental

The synthetic route of PTMA as an active material is shown in Fig. 2. First, the monomer of PTMA (2,2,6,6-tetramethylpiperidinyloxy-4-yl methacrylate) was synthesized by the esterification reaction of 4-hydroxy-2,2,6,6-tetramethylpiperidine-N-oxyl and methylmethacrylate (MMA) with a catalyst. Then the

* Corresponding author. Tel.: +81 3 5228 8749; fax: +81 3 5228 8749.
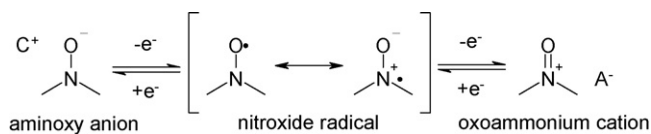*E-mail address:* komaba@rs.kagu.tus.ac.jp (S. Komaba).

Fig. 1. Redox reactions of nitroxide radical.

monomers were polymerized by adding Grignard reagent in toluene as solvent. The synthesized PTMA is partially cross-linked resulting in the insolubility into organic electrolyte solutions. The total reaction yield was sufficiently high for industrial application. Theoretical capacity of this cross-linked PTMA, therefore, is 108 mAh g^{-1} which was slightly smaller as compared with 111 mAh g^{-1} for non-cross-linked PTMA because of additional weight of crosslinking agent.

For preparation of working electrodes, the synthesized PTMA was milled sufficiently to reduce its particle size and thoroughly mixed with ketjen black (KB) (PTMA:KB = 2:1, w/w) by mechanical and solution method. For beaker-type cells, this PTMA/C composite (90 wt%) was mixed with a binder (10 wt%) such as polyvinylidene difluoride (PVdF) in N-methylpyrrolidinone and lithium polyacrylate (PAALi) or sodium polyacrylate (PAANa) in water. And for coin-type cells, this PTMA/C composite (85 wt%) was mixed with 10 wt% of PAALi as a binder and 5 wt% of carboxymethylcellulose (CMC) as a thickener in water. The obtained slurry was pasted onto stainless mesh (for beaker-type cell) or aluminium foil (for coin-type cell) by the doctor blade method. The obtained PTMA/C composite electrode was dried under vacuum at 80 °C prior to use, and the loading of PTMA on current collector was 1–1.5 mg cm^{-2} which is independent of binder and thickener. Beaker-type and coin-type (diameter: 20 mm, thickness: 3.2 mm) electrochemical cells, which were consisted of the above PTMA/C composite electrode as a working electrode and a lithium foil as counter and reference electrodes, were assembled in an Ar-filled glove box. The used electrolytes were 1 mol dm^{-3} LiClO$_4$ in EC:DMC (1:1, v/v) for a beaker-type cell and 1 mol dm^{-3} LiPF$_6$ in EC:DMC (1:1, v/v) for a coin-type cell. In case of coin-type cell, the separator material was polypropylene, and its thickness was 25 μm. Galvanostatic charge/discharge tests of the PTMA/C composite electrode were carried out between 2.5 and 4.2 V vs. Li$^+$/Li at room temperature. For the cycle performance test, the PTMA/C composite electrode was charged and discharged at 20C rate (1C corresponds to a current density, 108 mA g^{-1}, to charge or discharge its theoretical capacity for 1 h), and in the rate capability measurement, the electrode was charged at 1C rate and discharged at 1–50C rates. Cyclic voltammetry (CV) was performed using a beaker-type cell at room temperature between 2.5 and 4.2 V vs. Li$^+$/Li at various scan speeds. AC impedance measurements were carried out using a beaker-type cell at room temperature. The frequency range was 10^5 to 10^{-2} Hz with an AC amplitude of 10 mV.

Electron spin resonance (ESR) spectroscopy was performed to evaluate the purity of the synthesized PTMA based on the
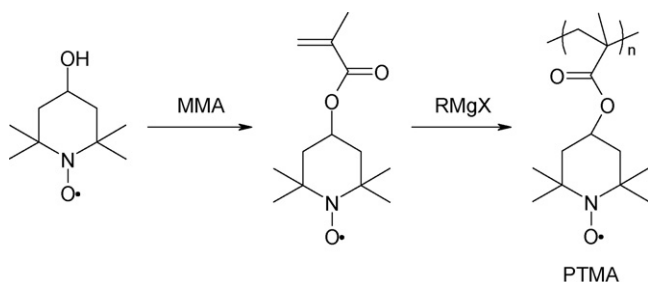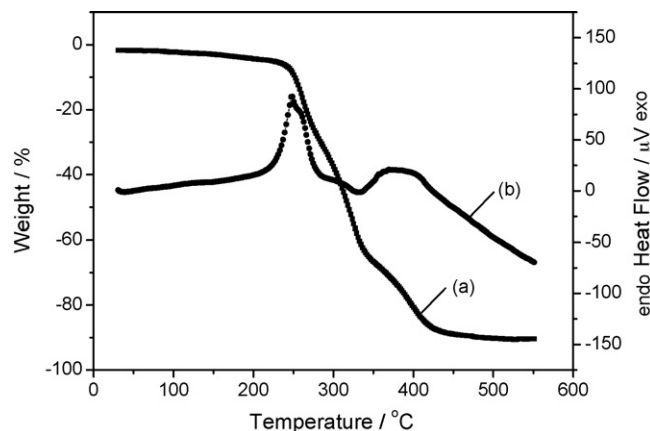

Fig. 2. Synthetic route of PTMA.

Fig. 3. (a) TG and (b) DTA curves of the synthesized PTMA at a rate of 10 °C min^{-1}.

radical density. To evaluate the thermal stability of the synthesized PTMA, thermogravimetry and differential thermal analyses (TG–DTA) were performed in argon atmosphere at a heating rate of 10 °C min^{-1} from 30 °C to 550 °C. Surface morphology was observed by scanning electron microscopy (SEM). Inductively coupled plasma (ICP) analysis of the PTMA/C composite electrode with PAALi as a binder in a beaker-type cell was performed after fully charging at 1C rate.

3. Results and discussion

Generally, active electrode materials must be insoluble in electrolyte solutions. Thanks to the crosslinking structure, the PTMA obtained by the synthesis was confirmed to be completely insoluble in ordinary carbonate-based solutions, e.g. ethylene carbonate and dimethyl carbonate. From ESR measurements, its radical concentration was equal to the value calculated from its chemical formula, showing that the obtained PTMA product contained no undesired impurities.

TG-DTA measurement was carried out to evaluate the thermal stability of the synthesized PTMA. Fig. 3 shows the TG-DTA curves of the synthesized PTMA. From DTA curve, an exothermic peak was observed around 250 °C, simultaneously, weight decreases considerably from TG curve, which is due to the thermal decomposition of PTMA. At 225 °C, its original weight was maintained over 95% from TG curve. This result proves that PTMA has sufficient thermal stability as an active electrode material for the application of electrochemical energy storage devices though the material consists of organic polymer compounds combined with organic radicals.

The SEM images of the synthesized PTMA with and without carbon mixing are shown in Fig. 4. Fig. 4a shows that the synthesized PTMA after milling has a flake-like morphology and its particle size is less than 10 μm. Fig. 4b shows the photo of PTMA/C composite obtained by mechanically mixing PTMA with ketjen black as a conductive assistant (PTMA:KB = 2:1, w/w). It reveals that the original particles of the radical polymer are uniformly coated and modified with tiny particles of ketjen black.

Fig. 5 shows the charge and discharge curves and its variation in discharge capacities of the PTMA/C composite electrode with PAALi as a binder in a beaker-type cell in which long cycle measurements is free of the problems associated with the dendrite deposition on lithium anode. The PTMA/C composite electrode was charged and discharged at high current density of 20C rates. Clearly, the PTMA/C electrode exhibited highly reversible redox performance at approximately 3.6 V with rather small polarization in spite of 20C rate, and the capacity based on the PTMA mass was around 85–90 mAh g^{-1}. Because of successful modification of
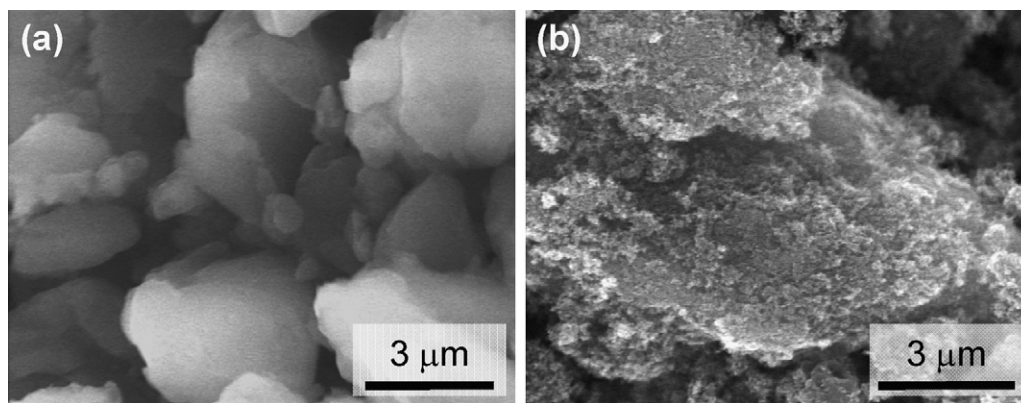
Fig. 4. SEM images of (a) synthesized PTMA after milling and (b) PTMA/C composite (PTMA:KB = 2:1, w/w).
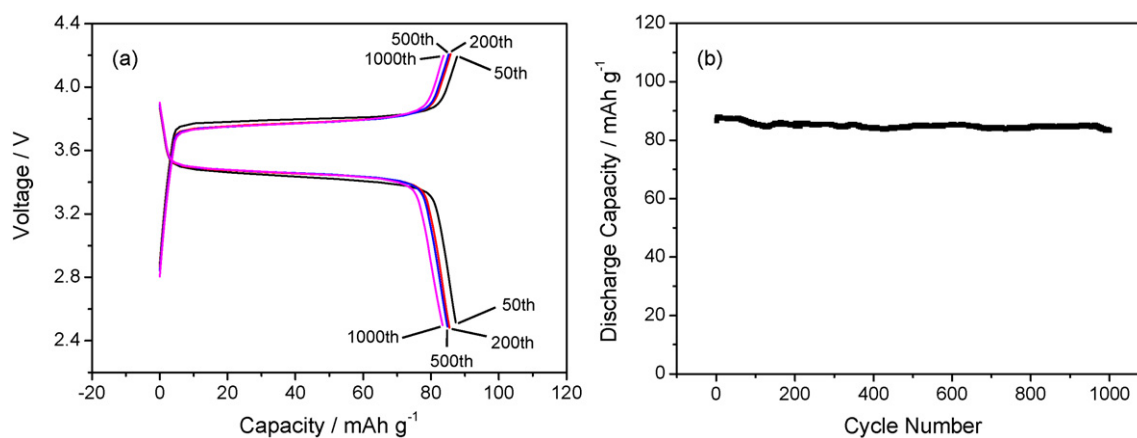

Fig. 5. (a) Galvanostatic charge and discharge curves of the PTMA/C composite electrode with PAALi as a binder and (b) variation in discharge capacity over one thousand cycles.

PTMA with carbon as mentioned in Fig. 4, the electric conduction was expected to be improved in the PTMA/C electrode though the original PTMA possesses electronically insulating character. Note that the electrode retained 96% of the initial capacity over 1000 cycles, supporting almost no capacity fading, while the transition metal oxides as positive electrode in Li cell usually show much capacity fading after 1000 cycles from our experiences [12,13]. We obtained the almost identical electrochemical performance for the PAALi and PAANa used as a binder. It is likely that this high cycle performance is attributed to the fact that the redox of PTMA is a simple reaction to form the oxoammonium salt doped with anions

(ClO_4^-) in the electrolyte. Since we used the polyanion of PAALi as a binder, there are two possibilities for charge compensation in the p-type redox of PTMA, that is, perchlorate anions in the electrolyte and carboxylic anions originated from polyacrylate in the electrode. The latter case was observed for the composite of polypyrrole/poly(styrenesulfonate) and polypyrrole/polyacrylate [14]. If the carboxylic anions of PAALi act as counter anions, the Li content in the electrode should decrease by releasing Li^+ from PAALi to electrolyte solution during charging process of PTMA. However, ICP analysis revealed no changes in the Li content in the electrode after/before charging process. Consequently, the
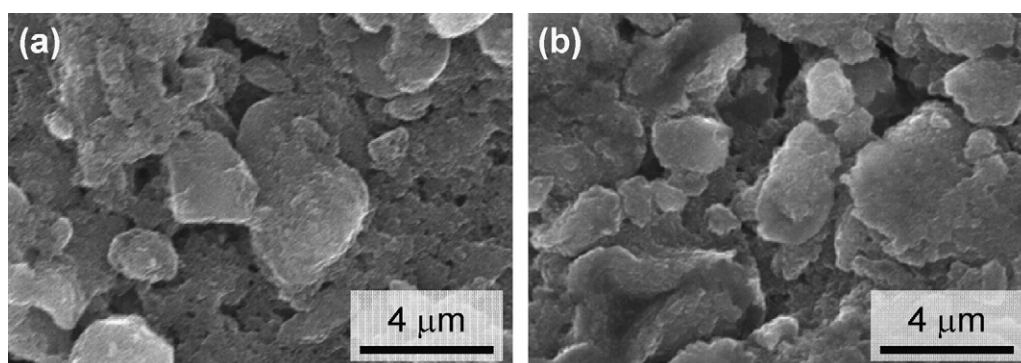

Fig. 6. SEM images of the PTMA/C composite electrodes (a) before and (b) after charge/discharge test of 1000 cycles.
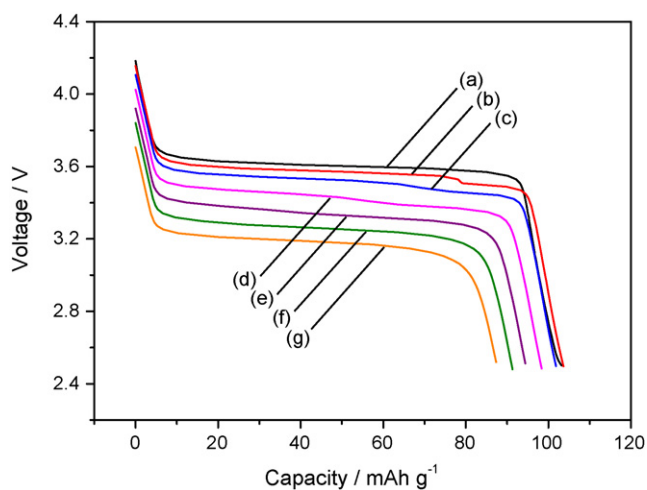
Fig. 7. Discharge rate dependence of the PTMA/C composite electrode with PAALi binder after fully charging at 1C. Discharge rates: (a) 1C, (b) 5C, (c) 10C, (d) 20C, (e) 30C, (f) 40C and (g) 50C.

carboxyl groups do not participate but the perchlorate anions in electrolyte participate in the p-type redox process of PTMA.

We also observed the morphology of the PTMA/C composite electrode before and after charge/discharge tests. The SEM images of the PTMA/C composite electrode with PAALi as a binder and CMC as a thickener are shown in Fig. 6. The SEM image before galvanostatic charge/discharge tests (Fig. 6(a)) shows the PTMA particles are coated with ketjen black clearly. Even after 1000 cycles of charge/discharge tests, no significant changes in the surface morphology was observed as compared with that before charge/discharge tests. It is most likely that the remarkably stable morphology was due to the unchanged main chain of PTMA polymer during redox as redox center is localized at side chain group of the PTMA (see Figs. 1 and 2). This unaffected morphology agrees well with the long cycle life in Fig. 5.

Fig. 7 shows the discharge rate capabilities of the PTMA/C composite electrode with PAALi as a binder in a beaker-type cell. The charging process of the electrode was carried out at 1C rate, and the following discharge was carried out at 1–50C rates. When the PTMA/C composite electrode was discharged at 1C rate, a plateau was observed at 3.61 V and the discharge capacity was 103 mAh g^{-1}, almost corresponding to its theoretical capacity of 108 mAh g^{-1}. This result indicates that almost all nitroxide radicals in the PTMA are oxidized to oxoammonium cations in charge process and reversibly reduced to nitroxide radicals in discharge
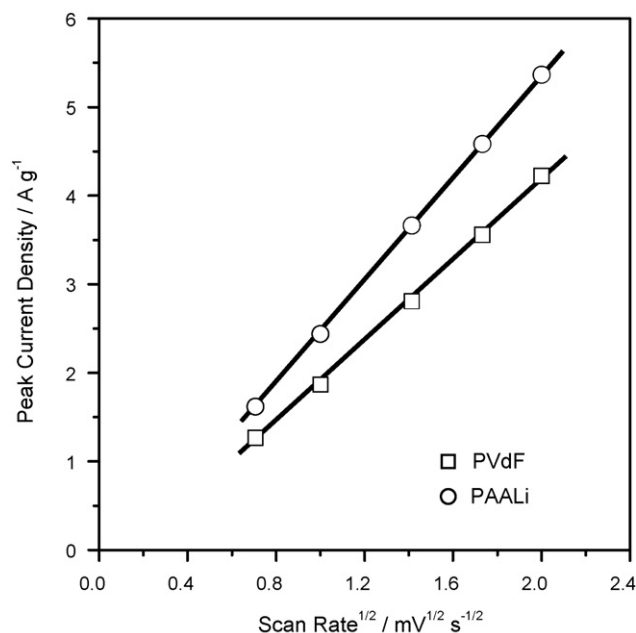

Fig. 9. Relation between anodic peak current density and square root of scan rate for PTMA/C electrodes with PVdF and PAALi binders.

process. When the PTMA/C was discharged at higher C rates, it showed 87 mAh g^{-1} even at 50C rate, corresponding to 81% of its theoretical capacity. And, there appeared to be small iR drops at higher C rates (e.g. 3.19 V at 50C rates) because of the suppression of electrochemical polarization compared to the conventional Li-ion electrode and the previous organic radical electrodes [7,10]. This superior rate capability of the PTMA/C composite was attributed not only to the fast electron-transfer kinetics of the TEMPO radical [3,11] but also to the uniform conduction path of electron and doping anion throughout the PTMA electrode by mixing with carbon with polyacrylate binder.

Fig. 8 shows cyclic voltammograms of the PTMA/C composite electrodes with PVdF or PAALi as binders in beaker-type cells. Cyclic voltammetry was performed using beaker-type cells with three-electrode configuration at room temperature between 2.5 and 4.2 V vs. Li$^+$/Li at different scan rates. In both cases using different binders, the anodic current density and total quantity of charge passed are nearly equal to those of cathodic scan, indicating the reversible redox reaction and sufficient coulombic efficiency of PTMA. And the potentials, at which anodic and cathodic peaks appeared, become
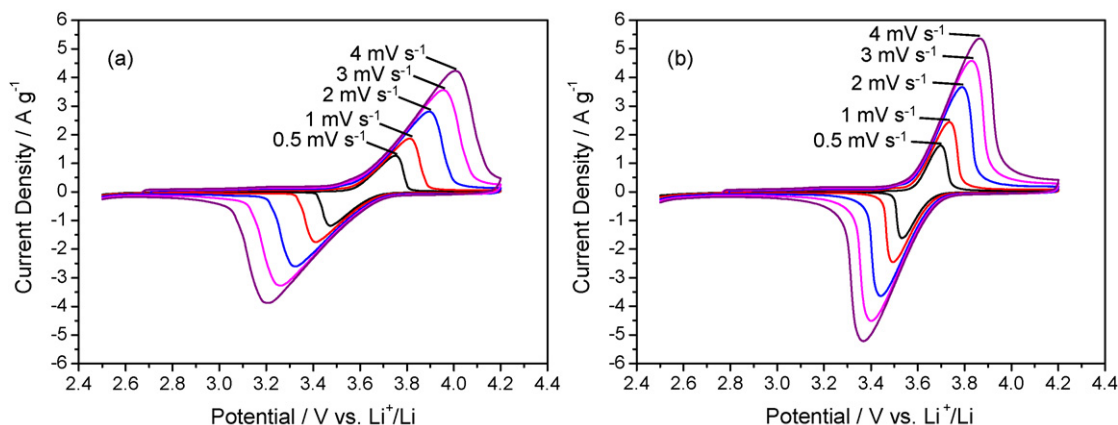

Fig. 8. Cyclic voltammograms of the PTMA/C composite electrodes with (a) PVdF and (b) PAALi binder.
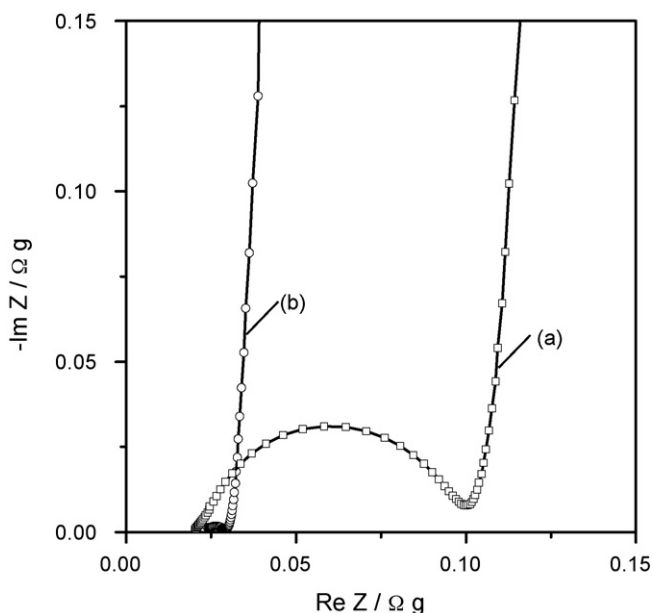
Fig. 10. Cole–Cole plots of the PTMA/C composite electrodes with (a) PVdF and (b) PAALi as a binder. The frequency range was 10^5 to 10^{-2} Hz.

distant from each other by increasing scan rates due to increase of the electrochemical polarization for both binders. However, the degree of the electrochemical polarization is different. When PAALi is used as a binder, the electrochemical polarization was successfully suppressed as compared with the PVdF binder. We also confirmed the similar suppressed polarization for the PAANa electrode.

From these voltammograms, the plots of anodic peak current densities vs. square root of scan rate are shown in Fig. 9. Obviously, the anodic peak current densities are in proportion to square root of scan rate in both cases of PVdF and PAALi. This indicates that the rate-determining step of the redox reaction is a diffusion process of the dopant anions. Of course, the larger slope with higher current density was obtained for the PAALi electrode, showing the fast diffusion of the anions within the electrode. When polyacrylate powders was put into EC:DMC solution containing lithium salts, the jelly like-precipitation was visually confirmed and it became turbid solution, indicating that alkali polyacrylates is not insoluble in the electrolyte. In case of the polyacrylate electrode, therefore, the electrolyte solution should be partly penetrated into the PAALi

electrode to improve the dopant diffusivity, resulting in the higher kinetics of the redox reaction of the radical polymer.

Furthermore, AC impedance measurements were carried out to investigate the differences of the electrochemical polarization when different binders are used for the PTMA/C composite electrode. Beaker-type cells of three electrodes were used for the accurate measurements, and the frequency range was 10^5 to 10^{-2} Hz with an AC amplitude of 10 mV. Fig. 10 shows Cole–Cole plots of the PTMA/C electrodes with PVdF or PAALi as binders in beaker-type cells. From the intercept of the semicircle on Re Z axis, the values of solution resistance are rather similar in both cases. When we compare the diameters of the semicircle appearing in the higher frequency region, the PTMA/C composite electrode with PAALi as a binder showed much smaller diameter, indicating the lower resistance of charge transfer reaction than that with PVdF. This is attributed to the fact that polyacrylate binders (e.g. PAALi and PAANa) are swollen by organic carbonate electrolyte, like formation of jell as mentioned above, resulting in the increase of the surface area contacting the electrolyte. Thus the electrode with PAALi demonstrated lower charge transfer resistance than that with PVdF, so that the suppressed polarization was observed for the polyacrylate binders.

Since the PTMA electrode itself shows excellent rate capability by using polyacrylate binders, the solutions resistance is expected to be not negligible to determine the essential rate capability. Therefore, we tested discharge rate capabilities without and with a reference electrode galvanostatically, and evaluated the iR drop of the PTMA/C composite electrode. Fig. 11 shows the discharge rate capabilities of the PTMA/C with PAANa binder in a beaker-type cell. In case of three-electrode configuration with reference electrode, the solution resistance was reduced because of the close distance negligible current flow between reference and PTMA electrode. The charging process of the electrode was carried out at sufficiently slow rate of $1C$, and then the discharging process was carried out at 1–$50C$ rates. In the case of the two-electrode cell without a reference electrode (Fig. 11(a)), the discharge voltage drops considerably at higher C rates because of larger iR drop of the solution resistance between the PTMA/C and counter Li electrodes. But in the case of the three-electrode cell with a reference electrode, the iR drop was clearly suppressed in case of higher rate tests, resulting in improvement of power capabilities. We believe the general possibility that this high cycle stability and high rate capabilities of the PTMA/C composite will be satisfactory for high potential for the application to not only secondary batteries but also redox capacitors with aprotic electrolyte solution on the basis of the p-type redox reactions.
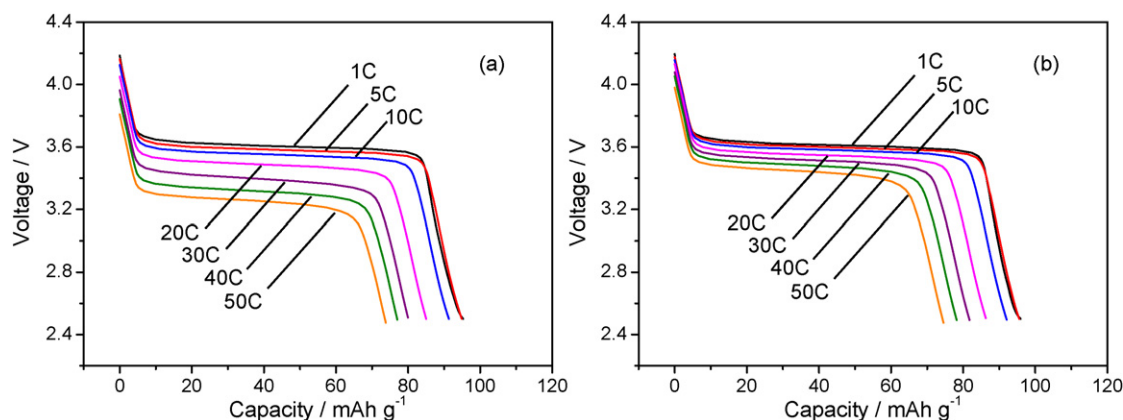

Fig. 11. Discharge rate capabilities of the PTMA/C composite electrode with PAANa as a binder: (a) two-electrode configuration with quasireference Li electrode and (b) three-electrode configuration with a reference electrode.

4. Conclusion

We tested the electrochemical performance of the PTMA/C composite electrode and demonstrate the fast redox performance by adopting carbon composite and polyacrylate binders. When the variation in discharge capacities of the PTMA/C composite electrode was tested galvanostatically at 20C rates, the electrode retained 96% of the initial capacity even after 1000 cycles, resulting from the fact that the redox of PTMA is a simple reaction to form the oxoammonium salt doped with ClO_4^- anions in the electrolyte without the stress of the chemical structure. When the PTMA/C composite electrode was discharged at different C rates, the electrode retained 81% of the theoretical capacity even at 50C rates. This high rate capability originates from the fast electron-transfer kinetic of the TEMPO radical and the improved conductivity throughout the electrode by mixing with carbon.

References

[1] K. Nakahara, S. Iwasa, M. Satoh, Y. Morioka, J. Iriyama, M. Suguro, E. Hasegawa, Chem. Phys. Lett. 359 (2002) 351.
[2] J. Iriyama, K. Nakahara, S. Iwasa, Y. Morioka, M. Suguro, M. Satoh, IEICE Trans. E85-C 6 (2002) 1256.
[3] H. Nishide, S. Iwasa, Y.J. Pu, T. Suga, K. Nakahara, M. Satoh, Electrochim. Acta 50 (2004) 827.
[4] M. Satoh, K. Nakahara, J. Iriyama, S. Iwasa, M. Suguro, IEICE Trans., E87-C 12 (2004) 2076.
[5] H.Q. Li, Y. Zou, Y.Y. Xia, Electrochim. Acta 52 (2007) 2153.
[6] K. Nakahara, J. Iriyama, S. Iwasa, M. Suguro, M. Satoh, E.J. Cairns, J. Power Sources 163 (2007) 1110.
[7] K. Nakahara, J. Iriyama, S. Iwasa, M. Suguro, M. Satoh, E.J. Cairns, J. Power Sources 165 (2007) 398.
[8] K. Nakahara, J. Iriyama, S. Iwasa, M. Suguro, M. Satoh, E.J. Cairns, J. Power Sources 165 (2007) 870.
[9] J.K. Kim, G. Cheruvally, J.W. Choi, J.H. Ahn, D.S. Choi, C.E. Song, J. Electrochem. Soc. 154 (2007) A839.
[10] J.K. Kim, G. Cheruvally, J.W. Choi, J.H. Ahn, S.H. Lee, D.S. Choi, C.E. Song, Solid State Ionics 178 (2007) 1546.
[11] T. Suga, Y.J. Pu, K. Oyaizu, H. Nishide, Bull. Chem. Soc. Jpn. 77 (2004) 2203.
[12] S.T. Myung, S. Komaba, N. Kumagai, J. Electrochem. Soc. 148 (2001) A482.
[13] S.T. Myung, K. Izumi, S. Komaba, Y.K. Sun, H. Yashiro, N. Kumagai, Chem. Mater. 17 (2005) 3695.
[14] T. Momma, S. Komaba, T. Osaka, S. Nakamura, Y. Takemura, Bull. Chem. Soc. Jpn. 68 (1995) 1297.